Journal of Research of the National Bureau of Standards—D. Radio Propagation
Vol. 63D, No. 1, July–August 1959

Power Requirements and Choice of an Optimum Frequency for a Worldwide Standard-Frequency Broadcasting Station

A. D. Watt and R. W. Plush

(January 15, 1959)

Calculations are presented for the expected transmission characteristics and atmospheric noise levels in the 8- to 100-kc band. When these are combined with carrier-to-noise requirements for a given precision of frequency comparison, it is indicated that a minimum radiated power in the order of 10 to 100 kw for frequencies in the vicinity of 20 kc will be required to provide worldwide coverage. Minimum observation times of 15 to 30 min appear to be required for these transmitter powers in order to obtain a precision of frequency comparison of 1 part in 10^9 for typical transmission paths. Carrier-to-noise requirements and the factors determining this ratio are considered for typical receiving systems.

1. Introduction

Observations by various investigators of the frequency stability of lf and vlf radio signals at great distances has led to the proposal by J. A. Pierce, et al. [1][1] for a single standard frequency transmitter with worldwide coverage. Descriptions of various radio systems employed for comparing frequency are given by Pierce [2], along with the stabilities obtainable. Other observations on frequency stability are reported by Allan, Crombie, and Penton [3], and some of the possible advantages of a vlf or lf frequency standard over the present high frequency transmissions from WWV are discussed by George [4].

It is the purpose of this investigation to make preliminary determinations of the optimum frequency and the power requirements for reliable coverage. The first objective will be to determine the radiated power required to provide this coverage as a function of frequency. Since the atmospheric noise level is well in excess of antenna or receiver thermal noise in this frequency range for reasonable sized antennas, we can write

$$P_r = -E_1 + E_{nm} + C/N_{1\,\mathrm{kc}} + T_x. \qquad (1)$$

All factors are expressed in db: P_r is the radiated power relative to 1 kw, E_1 is the field produced at the receiving location for 1 kw radiated relative to 1 μv/m, E_{nm} is the median rms noise field in a 1 kc band relative to 1 μv/m, $C/N_{1\,\mathrm{kc}}$ is the required rms carrier to rms noise in a 1 kc effective bandwidth for the type of service involved, and T_x is a factor which assures this type of service for a given percentage of all hours in spite of the time variability of the noise as well as the variation in carrier field strength due to propagation effects.

[1] Figures in brackets indicate the literature references at the end of this paper.

2. Carrier Field Intensity Calculations

Before calculating E_1 the field intensity anticipated for 1 kw radiated, we must first determine the distance to the areas most difficult to serve. With the aid of a globe and noise maps by Crichlow, et al. [5], it readily becomes apparent that for a transmitter located near the Boulder Laboratories in Colorado the most difficult service areas in terms of carrier-to-noise requirements will be in the vicinity of Java or Madagascar. The distance to these areas is approximately 17,000 km. The transmission paths are over both land and sea water, and this should be allowed for in the final calculations.

The large amount of recent theoretical and experimental work in the field of vlf propagation [6] has placed us in a position where relatively accurate predictions of field intensity can be made in this frequency range. Studies by Wait [7] have presented expressions for the vertical electric field which can be well approximated for ranges in excess of 2,000 km as

$$E \approx K + P_r - 10\log_{10} f(\mathrm{kc}) - 10\log_{10}[a\sin(d/a)] - \alpha d/1{,}000 \qquad (2)$$

$$d > 2{,}000 \text{ km},$$

where E is the vertical electric field in db relative to 1 μv/m at a distance d from the source, d is this distance in kilometers, K is a constant (see appendix A) which equals 97.5 for day paths assuming an ionospheric height of 70 km and equals 94.8 for night paths where $h=90$ km, P_r is the radiated power in db relative to 1 kw, f(kc) is the frequency in kc, a is the earth's radius ($\sim$6,400 km), and α is the attenuation rate in db per 1,000 km. All except the last term represent the unabsorbed field expected from the dominant mode being propagated between two concentric spherical shells. The term α, which

accounts for the fact that the shells are not perfectly conducting, will naturally vary with ionospheric conditions, ground conductivity, frequency, and perhaps to a small extent on direction of propagation with respect to the earth's magnetic field. Experimental determinations of the factor α can be made either by employing equation (2), or by observing the rate of decrease in E with distance relative to the (a sin d/a) factor. Determinations of both types have been made employing observations by Round et al. [8], Pierce [9] and Heritage [10], along with theoretical calculations by Wait [11] for both single and double layer ionospheric models, and the results presented in figure 1. It should be emphasized that

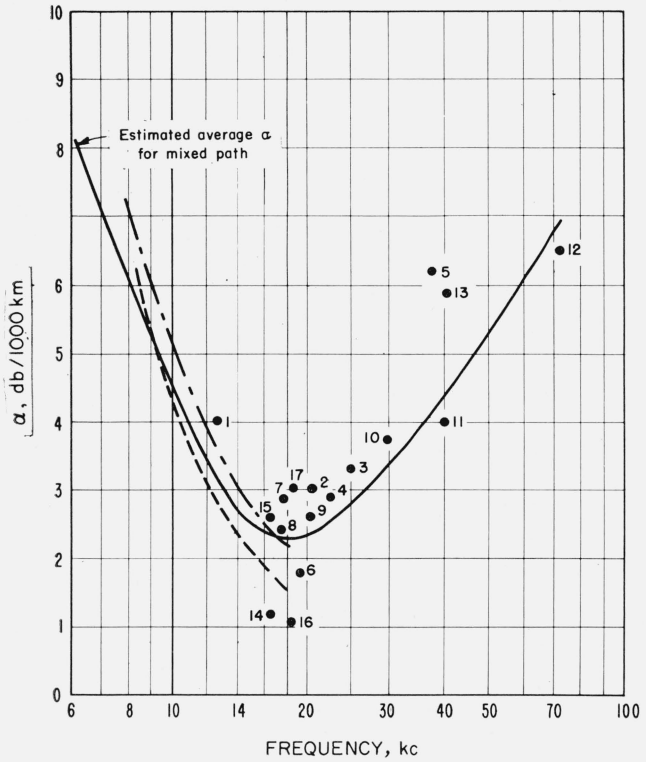

FIGURE 1. *Attenuation coefficient for daytime conditions*

No.	Author Ref.	Transmitter		Cosχ* Receiver	Path
1	Round, et al. [8]	LY		Dorset	L & S
2	do	POZ		do	L & S
3	do	LCM		do	L & S
4	do	KET		do	L & S
5	do	GB		do	L & S
6	do	YN		Boonah	L & S
7	do	LY		do	L & S
8	do	UFU		do	L & S
9	do	OUI		do	L & S
10	Pierce [9]	San Diego	0.96	Hawaii	S
11	do	do	.96	do	S
12	do	do	.96	do	S
13	do	do	.93	Wash., D.C	L
14	Heritage [10]	NPM		Aircraft	S
15	do	NPM		do	S
16	do	NLK		do	S
17	do	NLK		do	S
	Wait [11]	Theory		ground $\{\sigma=\infty$	
	do	do		$\sigma=2.2$ mmho/m	

L=Land
S=Sea
*Max. sun's zenith path midpoint

these attenuation rates are only approximate median values for low latitude paths with relatively few discontinuities and a fairly low percentage of land in the total path. Unfortunately, present knowledge in this field is not sufficient to permit extremely accurate predictions of α for all paths. It does appear, however, that α is considerably greater for high latitude paths when appreciable lengths of low conductivity earth surface such as permafrost or glaciers are involved. In addition, the total loss over a path appears to increase when appreciable discontinuities in surface conductivity and/or height of the ionosphere are present over the path. This last effect which occurs when a sunrise or sunset boundary is crossed by the path may cause an effective decrease in carrier field by approximately 6 to 10 db and 3 to 6 db respectively over some but not necessarily all paths.

Since α varies appreciably with ionospheric conditions, our estimated α in figure 1 is only expected to be near some median value. Experimental substantiation of the general shape of this curve in the low frequency region is given by atmospheric noise measurements [12] and by Taylor [13] in his spherics observations.[1] It should be pointed out that the nighttime attenuation values are expected to be more variable than the daytime values, and in addition α will not increase as rapidly with frequency above 18 kc at night as is shown for the day conditions.

The values of α from figure 1 are now employed in eq (2) for a 17,000-km path and an assumed radiated power of 1 kw. The results are shown in figure 2 where it is evident that at this distance the propagation path appears to have a rather narrow pass band centered around 18 kc.

So far we have not considered the affects near the antipode where the signal is arriving from essentially all directions. In theory, at this point the electric field focuses and an appreciable build up of some 20 db at 20 kc is possible. Observations in this area by Round, et al. [8] have shown that at times the measured field can be 20 db above that anticipated for a single path at this distance. Their observations also indicate, as would be expected, that beats are produced and that the received field is not very stable due to interference between the various paths. Some of this interference effect can possibly be reduced by loop and vertical antenna combinations or perhaps some type of angle diversity with loops. Fortunately, for a transmitting site near Boulder, the antipode is in the Indian Ocean where little use of the standard frequency broadcast service is presently anticipated.

The possibility of whistler mode propagation producing interference as shown by Helliwell [23] should also be considered; however, again the conjugate point from Boulder is not in an area of great importance.

[1] Additional material by Wait [25] on attenuation rates including an extensive bibliography has become available after this study was completed. In general, the attenuation rates indicated by Wait are in good agreement with figure 1, although it is evident that further careful experimentation is desired to determine with greater precision the shape of this curve and the frequency of minimum attenuation.

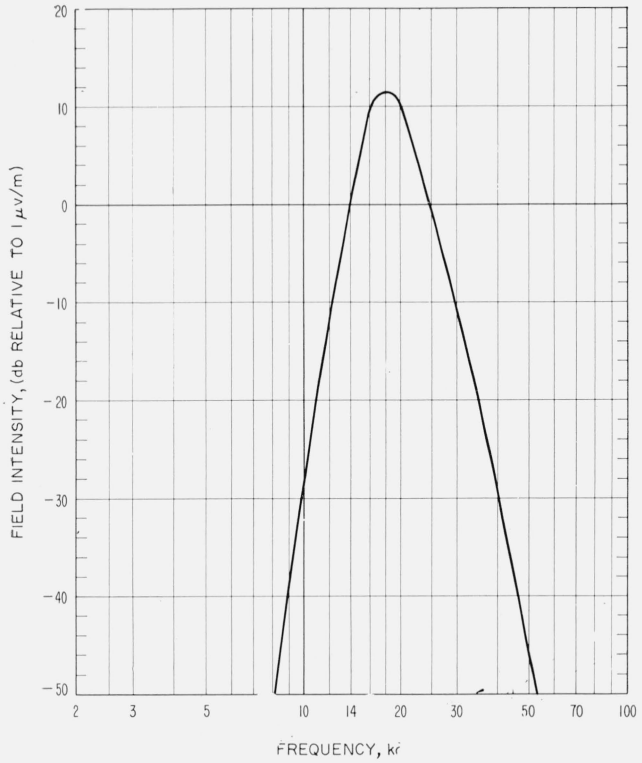

FIGURE 2. *Field intensity expected at 17,000 km for 1 kw radiated power.*

Daytime, mixed land and sea path: land ≈ 20 percent, sea ≈ 80 percent (average ionospheric conditions assumed). Calculations based on eq 2 and α of figure 1.

3. Atmospheric Noise Levels

The second term in eq (1), E_{nm} describes the median rms noise field in a 1-kc bandwidth, and values anticipated in the regions considered can be found in CCIR Report No. 65 [5]. The maximum level anticipated during the summer months corresponds to a noise grade of 90 db at 1 mc, and the anticipated median values in the frequency range considered are shown in figure 3. Since the high noise level results from local thunderstorm activity, and the predictions are extrapolated to 10 kc from higher frequency measurements, the shape of this curve has been slightly modified to agree with the average spectrum of the radiation component from lightning strokes [12]. In addition, several points have been included from an earlier paper [14] along with a typical winter curve [12].

4. Carrier-to-Noise Requirements

The ratio of rms carrier to effective rms noise in a 1-kc bandwidth, $C/N_{1\text{ kc}}$, is useful in defining the amount of carrier power required for a satisfactory determination of frequency. Pierce [2] has shown that several different types of equipment are presently employed for frequency comparison, and the actual $C/N_{1\text{ kc}}$ required will undoubtedly vary with the characteristics of the receiving equipment and

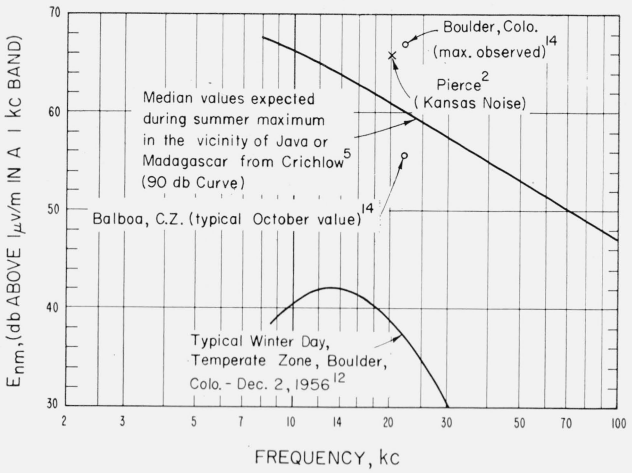

FIGURE 3. *Typical atmospheric noise field strengths.*

Rms values in a 1-kc effective bandwidth.

the amount of effort spent in attempting to separate the desired energy from the undesired noise energy.

It is well known that the carrier-to-noise ratio required to make a frequency comparison is dependent on the precision required and the period of time allowed to make the frequency comparison. The precision of frequency comparison is defined as $\epsilon = \sigma f_d / f$ where f is the standard frequency, and σf_d is the standard deviation of the frequency difference between the resultant received frequency and the standard frequency.[2] Since there is a definite minimum time required for a given precision of frequency comparison due to propagation path phase instabilities, we must consider this effect first. This effect is analyzed in appendix B where it is shown that the ϵ obtainable is independent of observing time for periods short compared to the carrier fade period and then becomes inversely proportional to this period for some systems. It also appears that for periods long compared to the carrier fading that some systems provide a decrease in ϵ which is proportional to the 3/2 power of time. Calculations in the 20-kc region indicate that frequency comparisons can be made with a precision of one part in 10^9 in observing periods of 15 to 30 min.

The factors which determine required $C/N_{1\text{ kc}}$ are considered in appendix C. The results are shown in figure 4 which gives anticipated values of $C/N_{1\text{ kc}}$ for several observing times. It is interesting to note here that if the carrier is required to carry information at an appreciable rate (such as 60 words/min) over an automatic teletype system, that the value of $C/N_{1\text{ kc}}$ may be approximately 18 db for 0.1 percent errors [15]. The very great increase in required powers for communication is readily seen.

[2] In order to conform with general usage, it should be noted that as the ability to accurately compare frequency increases, the value of ϵ actually decreases.

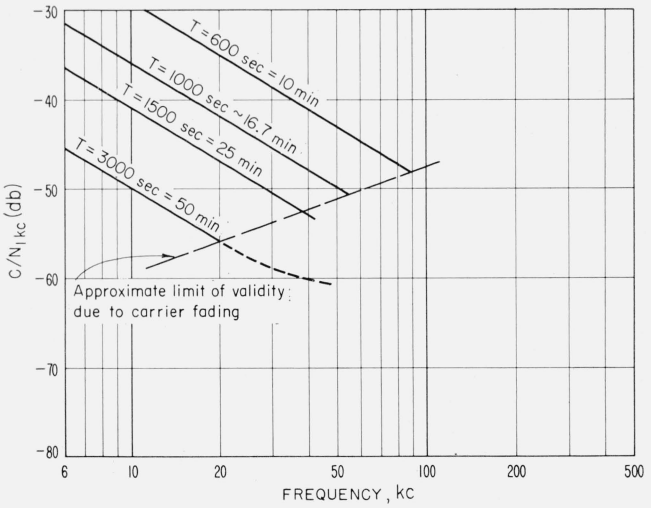

FIGURE 4. *Carrier-to-noise requirements as a function of frequency for a frequency comparison with a precision of 1 part in 10^9 in observing periods indicated, based on eq (C6).*

Eq (C6):

$$C/N_{1\,kc}(dt) = -106 - 20 \log \epsilon - 20 \log f_{kc} - 30 \log T,$$

where ϵ = required precision
f_{kc} = frequency in kc
T = observing period (seconds).
NOTE.—Equivalent receiver bandwidth $\approx 1/T$.

5. Calculations of Required Radiated Power

The next term in eq (1) is T_x, the allowance which must be made to provide the level of performance specified for a given percentage of all hours. A value of 90 percent of all hours was chosen as being reasonable for the type of service involved. T_{xn}, shown as the lower curve in figure 5, represents the additional allowance which must be made for the variability in atmospheric noise levels, and T_{xs} is the allowance for signal level variability. T_x is obtained by taking the square root of the sum of the squares of the individual variances of T_{xn} and T_{xs}. This yields the upper curve, and it can be noted that both the noise level and anticipated transmission loss variability combine to require a margin that increases with frequency above 20 kc. The inserted curve on figure 5 may be used to determine T_x for less than 90 percent of all hours. For example, where T_x for 90 percent of all hours is 10 db at 20 kc, T_x for 74 percent of all hours is 50 percent of T_x (90) or 5 db at 20 kc.

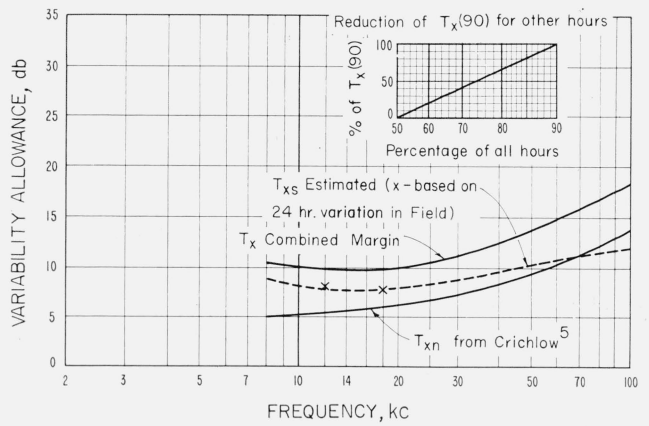

FIGURE 5. *Signal fading and noise variation margin for 90 percent of all hours.*

When all of these factors are properly combined, we obtain the curve shown in figure 6 which indicates minimum required radiated power at around 19 kc. It is interesting to observe that this low-loss vlf pass band is very close to the region where the majority of vlf transmitters are presently located.

The 2 kw of radiated power required for the 50-min observing period must be considered as a minimum value. It may be desirable to increase this value of radiated power to provide a margin of performance, and before a final choice is made, estimates should be prepared of the initial and operating costs versus radiated power for stations with capabilities ranging from 1 kw to 200 kw.

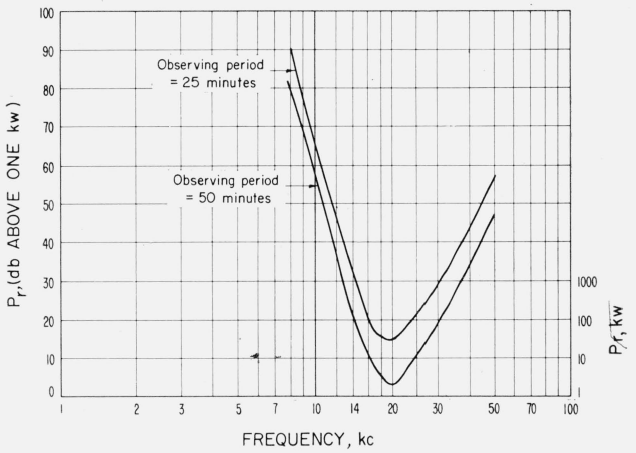

FIGURE 6. *Radiated power required for a worldwide standard frequency broadcasting station.*

Calculations based on a primarily daylight path of 17,000 km to the vicinity of Java or Madagascar (estimated most difficult service areas). Transmitter located near 40° N, 105° W.

6. Antenna Considerations

The factors involved in the design of an antenna to radiate economically the powers indicated in figure 6 are extremely complex. To give some idea of the effect of antenna characteristics on the choice of an optimum frequency, we can consider the transmitter power requirements based on the use of an antenna with properties similar to the NSS Annapolis, Md., antenna. The characteristics of this antenna expressed as antenna loss in decibels as a function of frequency are shown in figure 7. Although this is a rather complex antenna, consisting of nine 600-ft towers and capable of radiating approximately 200 kw at 20 kc, it can be shown that very similar loss characteristics could be obtained with a less expensive antenna if the radiated-power requirements were lowered.

Assuming the antenna characteristics in figure 7, we have shown by the curves in figure 8 the transmitter power required to furnish the service specified

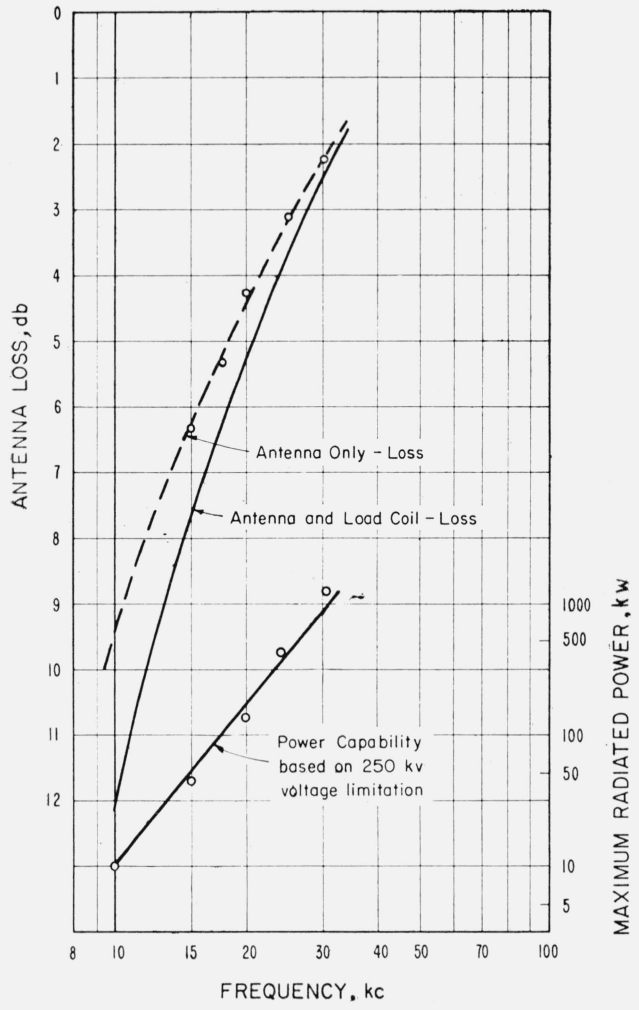

FIGURE 7. *Antenna power loss and maximum power capability.*

NSS Annapolis: nine 600-ft towers.

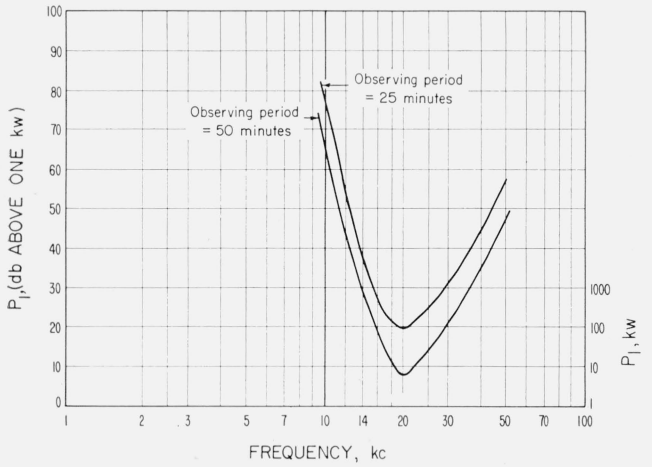

FIGURE 8. *Antenna input power requirements for a worldwide standard frequency broadcasting station.*

Calculations based on a primarily daylight path of 17,000 km to the vicinity of Java or Madagascar (estimated most difficult service areas). Transmitter located near 40° N, 105° W.

as a function of frequency. It should be emphasized that even if it were feasible to generate the powers which appear to be required at the lower frequencies, around 10 kc, that existing vlf antennas are not capable of radiating such powers due to corona limitations. This fact would be true of all known or planned antennas.

This voltage limiting effect which makes it more expensive to radiate a given amount of power as the frequency is decreased in this range must also be considered before a final choice of optimum frequency is made. It is not likely that this factor will increase the optimum frequency very much, but its influence should not be overlooked in a detailed study.

The authors are indebted to the following: K. A. Norton, J. R. Wait, W. W. Brown, F. M. Malone, A. H. Morgan, L. R. O. Storey, and W. D. George for helpful discussions and information; and to Mrs. W. Mau for her assistance in the preparation of the manuscript.

7. Appendixes

7.1. Appendix A: VLF Vertical Electric Field Intensity

Wait [7] has shown that the vertical electric field from a vertical current source can be written as

$$E_r = E_o \left[\frac{d/a}{\sin(d/a)} \right]^{1/2} \frac{(d/\lambda)^{1/2}}{h/\lambda} A/U, \qquad \text{(A1)}$$

where E_o is the field of the source on a perfectly conducting flat earth at a distance d from the source, d is this distance, a is the earth's radius, h is the height to the ionosphere, and λ is the wavelength, all in the same units. A/U represents a more complex expression in the original formula which in essence is the ratio between the actual field and the unattenuated field that would result if both earth and ionosphere were perfectly conducting spherical shells.

Using the well known relations

$$E_o = \frac{3 \times 10^5 \sqrt{P_r\,(\text{kw})}}{d\,(\text{km})}\ \mu\text{v/m}, \qquad \text{(A2)}$$

and

$$\lambda\,(\text{km}) = \frac{300}{f\,(\text{kc})}, \qquad \text{(A3)}$$

we can write

$$E_r = \frac{5.2 \times 10^6 \sqrt{P_r\,(\text{kw})}}{[a\ \sin(d/a)]^{1/2} \cdot \sqrt{f\,(\text{kc})} \cdot h\,(\text{km})} \cdot A/U. \qquad \text{(A4)}$$

where it is interesting to observe that if A/U remained constant, E_r would be inversely related to

h and $\sqrt{f}$. In the actual case A/U is a function of both of these factors. The complete expression for A/U involves the summation of many modes; however, at a distance in excess of 2,000 km, the first order mode is dominant and the attenuation can be expressed in terms of a simple exponential decay usually given in terms of α (decibels per 1,000 km). When this is employed and (A4) is expressed in logarithmic terms, we obtain eq (2).

7.2. Appendix B: Transmission-Path Phase Stability and Signal-Integration Times Required for Specified Frequency-Comparison Precisions

When a standard frequency broadcast is propagated via the ionosphere, Pierce [2] has shown that the diurnal changes of ionosphere heights, as well as the apparent roughness of the ionosphere, introduce effective transmission time variations. These variations in propagation time introduce phase variations on the received carrier, and the differential of these phase variations with respect to time represent the apparent instantaneous frequency deviations of the received carrier from the standard broadcast frequency.

The present state of the art in oscillator development has reached a point where these instantaneous frequency deviations introduced by propagation are considerably greater than the instabilities of the oscillator itself. Therefore, it becomes necessary to devise methods of reducing the effect of these propagation path induced frequency variations when accurate comparisons of frequency are desired. It has been shown by Pierce [2] that increasing the time of observation permits a more precise frequency comparison, and it is the purpose of this analysis to describe some of the factors involved in the amount of precision which is obtainable in a given length of time.

We shall first assume a very stable oscillator at the transmitting location with a frequency f_s. At the receiving location the frequency received f_r is not necessarily equal to f_s since the propagation path introduces a delay which varies with time. This variation in delay can be separated into a large diurnal variation with a smaller random component [2]. The standard deviation of this latter component expressed in degrees is defined as σ_Ω where typical values from Norton [16] are shown in figure 9 as a function of frequency for a single-hop path.

Assuming a condition where the diurnal phase is constant, the output of a phase detector at the receiving location relative to a highly stable local frequency source, will have the form shown in figure 10. The average observed frequency difference between the local oscillator f_l and the received carrier f_r will depend on the type of observation made.

Case I: The instantaneous frequency as derived by Carson [21] is the time derivative of phase, and the instantaneous frequency difference between f_l and f_r is

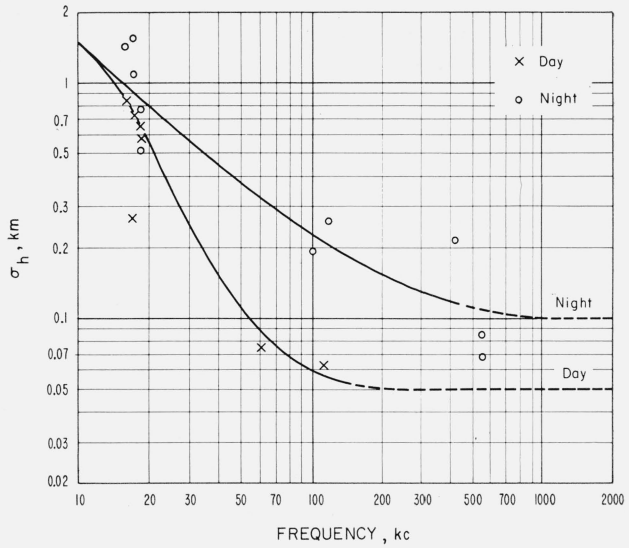

FIGURE 9. *Median effective ionospheric roughness parameter, σ_n, obtained from observations of σ_Ω,* σ_Ω (degrees) $\equiv 2.4\ f_{kc}\ cos\ \phi_i\ \sigma_h$ (km).

(See table B1 for sources)

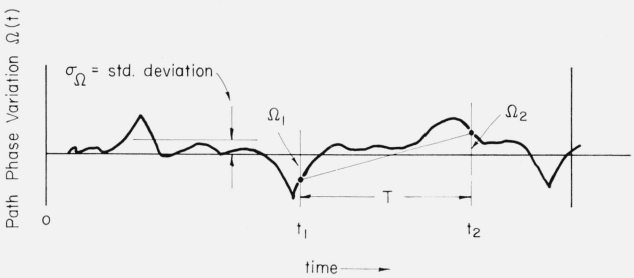

FIGURE 10. *Transmission-path phase variation.*

$$f_d\ (\text{instantaneous}) = \frac{1}{360} \cdot \frac{d}{dt}\ \Omega(t), \qquad \text{(B1)}$$

where f_d is in cps and $\Omega\ (t)$ is the phase difference in degrees between the carrier field at the receiver and a constant local reference. Measurements employing an instantaneous comparison of f_l and f_r will obviously have large excursions and, in view of this, we can consider averaging over a given interval T as shown in figure 10.

Case II: If the receiving system only sampled $\Omega\ (t)$ at times t_1 and t_2, we would obtain

$$f_d\ (\text{avg}) = \frac{\Omega_2 - \Omega_1}{360\ T}. \qquad \text{(B2)}$$

When T is short compared to the average carrier amplitude fade or phase variation period, τ, $f_d(\text{avg}) = f_d$ (instantaneous); while if T is long compared to a fade, Ω_1 and Ω_2 are independent. If the standard deviation of the received carrier phase σ_Ω is known, we obtain a total phase variance of $\sqrt{2}\ \sigma_\Omega$ and as a result

$$\sigma f_d\ (\text{avg}) = \frac{\sqrt{2}\sigma_\Omega}{360\ T}, \quad T > \tau \qquad \text{(B3)}$$

where σf_d (avg) is the standard deviation of the average frequency difference over a period T from the true transmitted frequency.

Case III: A more desirable type of observation would be to integrate Ω (t) over each consecutive period T such that the standard deviation of Ω out of the integrator at the end of each period is [22]

$$\frac{\sigma_o}{\sigma_i} \approx \frac{0.7}{\sqrt{T/\tau}}, \quad T/\tau > 1 \tag{B4}$$

where τ is the average fade period of the received carrier. Using this type of observation and combining (B3) and (B4) we obtain

$$\sigma f_d \text{ (integrated avg)} \approx \frac{\sigma_\Omega \tau^{1/2}}{360\, T^{3/2}}, \quad T/\tau >> 1. \tag{B5}$$

This standard deviation of frequency difference can be used to obtain the precision of frequency comparison, ϵ, where

$$\epsilon = \sigma f_d / f_1. \tag{B6}$$

In all cases, we will consider the phase for a single ray path and assume that the phase variation will increase directly with the square root of the number of ionospheric reflections m. It is also assumed that these paths are near grazing incidence which produces a minimum value for cos φ_i of 0.15 where φ_i is the angle of ionospheric incidence. Employing these assumptions we obtain from figure 9

$$\sigma_\Omega \text{ (deg)} = 360 \times 10^{-6} \sqrt{m} \cdot f \cdot \sigma_h. \tag{B7}$$

Since in eq (B1) σ_Ω is not given, we can observe that for phase variations of the type considered

$$\sigma f_d = \frac{k \sigma_\Omega}{360 \tau} \tag{B8}$$

where τ is the average fade or phase variation period and experience has indicated values for k in the order of 4.

Combining eq (B6) and (B7) with (B8), (B3), and (B5), respectively, we obtain the following precisions for each of the three cases considered.

Case I—instantaneous precision

$$\epsilon_1 \approx \frac{k \sqrt{m} \cdot \sigma_h}{10^6 \tau}, \quad (T < 0.1\tau). \tag{B9}$$

Case II—average precision

$$\epsilon_2 = \frac{\sqrt{2} \cdot \sqrt{m} \cdot \sigma_h}{10^6 T}, \quad (T > 3\tau). \tag{B10}$$

Case III—integrated average precision

$$\epsilon_3 = \frac{\tau^{1/2} \cdot \sqrt{m} \cdot \sigma_h}{10^6 T^{3/2}}, \quad (T > 3\tau). \tag{B11}$$

Since the average fade duration τ is required in cases I and III, an estimate of τ over the frequency range in question is given in figure 11. Combining these values with those obtained from figure 9, we obtain the estimated precision obtainable over a 17,000-km path at 20 and 50 kc, neglecting noise, shown in figure 12. The solid curves are experimental values from Pierce [2] for a somewhat shorter path. The single ray path analysis in effect implies that ϵ will increase with the square root of path distance. Actual data on the distance effect is unfortunately not available; however, it is expected that in the 20-kc vlf region and for long paths several ray paths will combine so as to reduce the fluctuations in phase. This will reduce ϵ below the values indicated for the single ray path.

It is interesting to observe that in the 16- to 20-kc region and for large values of T, ϵ is proportional to $1/T$. This probably results since the periods required are so long that the path phase is not independent of diurnal phase effects and eq (B11) does not apply. In the 50- to 60-kc region T is greater than 3τ for periods less than 20 min. As a result eq (B11) can apply. From Pierce's observations it is also seen that for large values of T, ϵ is now proportional to $1/T^{3/2}$.

TABLE B–1. *Estimates of the variance of phase on ionospheric paths*

No.	Frequency	Distance	Source	Time	Month	$\sigma_{obs.}$	S	$\sqrt{2(1-\rho)^2}$	σ_Ω	Mode	cos ϕ	σ_h
	kc	*Statute miles*				*Degrees*	λ			*m*		km_1
1	16	3,230	Pierce [2]	Day	February	8.06			8.06	3	0.146	0.829
2	16	3,230	do	Night	do	16.1			16.1	3	.170	1.424
3	17.2	640	Redgment [17]	Day	September	1.9	10	1.00	1.9	1	.174	0.265
4	17.2	640	do	Night	do	9.3	10	1.00	9.3	1	.206	1.093
5	17.2	640	do	Day	January	5.2	10	1.00	5.2	1	.174	0.726
6	17.2	640	do	Night	do	13.3	10	1.00	13.3	1	.206	1.563
7	18.4	3,488	do	Day	June and July	7.1	10	1.00	7.1	3	.144	0.643
8	18.4	3,488	do	Night	do	10.0	10	1.00	10.0	3	.169	.775
9	18.4	3,488	do	Day	December	6.5	10	1.00	6.5	3	.144	.588
10	18.4	3,488	do	Night	do	6.5	10	1.00	6.5	3	.169	.503
11	60	3,230	Pierce [2]	Day	do	2.8			2.8	3	.146	.077
12	100	2,350	Doherty [18]	Night	April	10.8	>40	1.41	7.64	1	.165	.193
13	115	780	Florman [19]	do	March	13.3	11	1.00	13.3	1	.189	.255
14	115	780	do	Day	do	2.7	11	1.00	2.7	1	.158	.062
15	418	1,250	do	Night	do	51	41	1.41	36.1	1	.167	.216
16	543	380	Brennan [20]	do	January to April	34	3.39	0.83	41.0	1	.371	.085
17	556	454	Redgment [17]	do	April and May	19	1.85	0.63	30.2	1	.334	.068

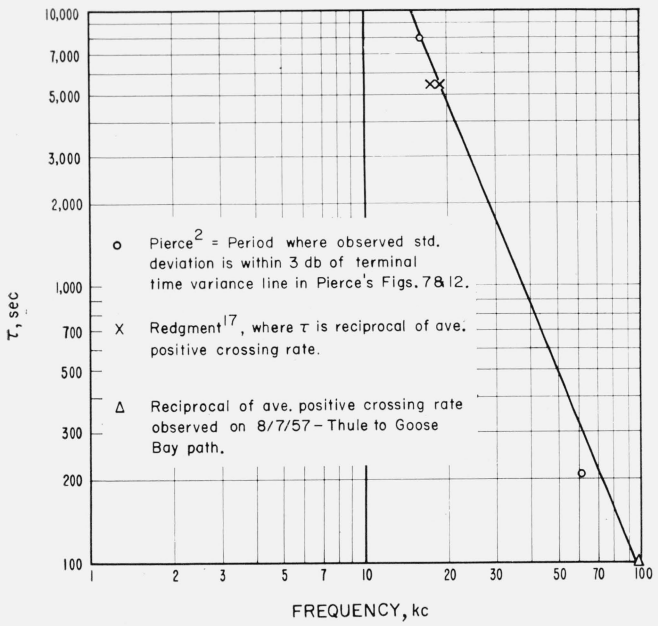

FIGURE 11. *Estimated fade period τ for a long distance daytime path* d$>$10,000 *km.*

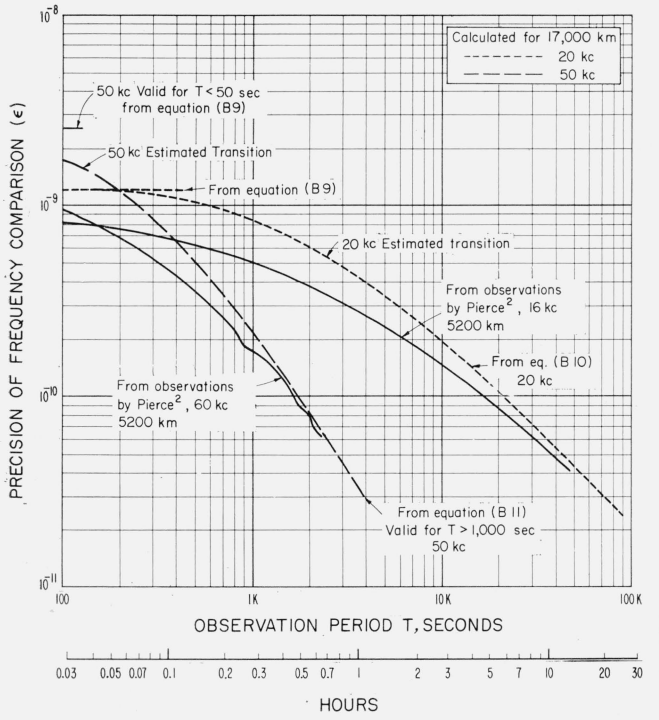

FIGURE 12. *Calculated precision of frequency comparison obtainable for a* 17,000*-km daytime path.*

Theoretical curves based on ionospheric roughness given in figure 9, estimated fade period τ given in figure 11, and an assumed $m=7$ ionospheric reflections.

7.3. Appendix C: Carrier-to-Noise Requirements for Precise Frequency Measurement

In all physical measurements there is a noise level which limits the degree of precision with which a given measurement can be made. The precision of frequency measurement can be determined from the precision with which a given number of degrees of carrier phase rotation can be measured. For example, if a carrier is contaminated with a small amount of narrow-band noise, the maximum phase variation of the resultant is $\phi_{max}=n/c$ where n and c are peak noise and carrier values. If we now desire the standard deviation of phase σ_ϕ, we can replace n with N and c with $\sqrt{2}\ C$ and obtain

$$\sigma_\phi \approx \frac{1}{\sqrt{2}}\frac{N}{C}, \tag{C1}$$

where C and N are the rms carrier and noise voltages [24].

If we now assume that our true period is $2\pi r$ radians where r is the number of whole cycles in our observing period and since ϕ is normally distributed, the total uncertainty or phase jitter is $\sqrt{2}\ \sigma_\phi$ radians, and the precision is given by

$$\epsilon=\sqrt{2}\sigma_\phi/2\pi r,$$

or we can express the precision obtainable as

$$\epsilon \sim \frac{N/C}{2\pi r}, \quad C/N \gg 1. \tag{C2}$$

If we now consider a receiving system where we integrate the phase output over an observing period, T, and compare it with the integrated value of the preceding period as in eq (B4), we obtain a reduction in phase jitter of approximately $(T\cdot BW)^{-1/2}$ as long as $T>1/BW$, where BW is the effective rf bandwith of the receiver before the final integration. Employing this correction to (C2), and observing that $r=T\cdot f$, where T is the period of measurement in seconds and f is the frequency in cycles per second, we obtain

$$\epsilon \approx \frac{N/C}{2\pi f T^{3/2} BW^{1/2}}. \tag{C3}$$

It should be emphasized that this expression applies only to the type of observation described, and it is not necessarily equal to the optimum obtainable.

Before employing (C3) we must be sure that inaccuracies of measurement which can occur in some systems do not arise due to a miscount of a whole cycle. This requirement is met by being sure that the noise envelope is less than the carrier for a specified percent of all time. Since the noise envelope is Rayleigh distributed, a protection of 1,000 to 1 is obtained with $C/N=8.5$ db, and 10,000 to 1 with 9.6 db. The actual probability of having the noise envelope remain below the carrier envelope for a

whole period T is found by taking the probability of one independent sample being correct and raising it to a power determined by the total number of independent samples which could be made in the whole sample. This power is approximately equal to $BW \cdot T$ which for a BW of 0.01 cps, and a T of 1 hr is 36. If we choose the $C/N = 8.5$ db case, we must raise 0.999 to the 36th power which yields a 96.7 percent probability of being free from errors of a whole cycle or more. It should be pointed out that this requirement which in effect places a threshold on the C/N in the receiver pass band is not always necessary since it is possible to locally introduce the correct number of whole cycles if the local standard is approximately correct.

Returning to (C3) and expressing C/N in decibels, we can write

$$C/N \text{ (db)} \approx -76 - 20 \log \epsilon - 20 \log f(\text{kc}) - 30 \log T - 10 \log BW. \quad \text{(C4)}$$

Since many different receiver combinations can be employed, it is desirable to obtain our results in terms of the rms carrier to rms noise in a 1-kc bandwidth expressed in decibels which is obtainable from

$$C/N_{1\text{kc}} = C/N \text{ (db)} - 10 \log \frac{1{,}000}{BW}, \quad \text{(C5)}$$

where BW is the receiver bandwidth in cycles per second. Combining (C4) and (C5) we obtain

$$C/N_{1\text{kc}} \approx -106 - 20 \log \epsilon - 20 \log f(\text{kc}) - 30 \log T, \quad \text{(C6)}$$

where it is seen that for a coherent type of detection the results are independent of receiver IF bandwidth. Typical ranges of $C/N_{1\text{kc}}$ for a precision of frequency comparison of one part in 10^9 are shown as a function of T in figure 13, and as a function of f in figure 4.

When T approaches the carrier fade period τ, described in appendix B, the effective carrier amplitude is reduced and (C6) no longer holds. In fact when T is several times τ, it is expected that the last term in (C6) will approach a decrease of 10 db per decade rather than 30. Since this effect is quite complex, including the shape of the power spectrum of the received field, we have only shown estimated $C/N_{1\text{kc}}$ values by dashed lines in this region. In addition, diurnal effects are expected to limit the validity of all these curves to values less than 15-K sec.

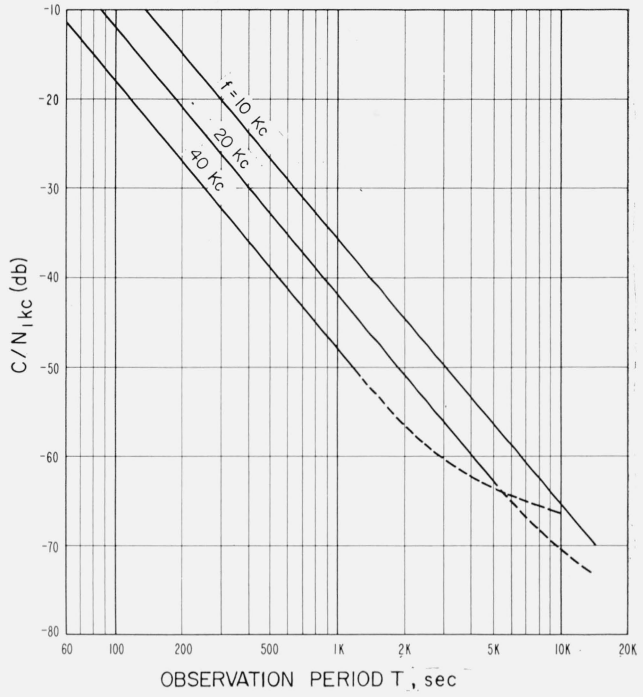

FIGURE 13. *Calculated carrier-to-noise requirements for a frequency comparison with a precision ϵ of 1 part in 10^9 in a period of T seconds.*

Calculations based on eq (C6):
$C/N_{1\text{kc}}(db) = -106 - 20 \log \epsilon - 20 \log f_{\text{kc}} - 30 \log T$
where: ϵ=required precision
f_{kc}=frequency in kc
T=observing period (seconds).

8. References

[1] J. A. Pierce, H. T. Mitchel, and L. Essen, World-wide frequency and time comparisons by means of radio transmissions, Nature **174,** 922 (1954).

[2] J. A. Pierce, Intercontinental frequency comparison by vlf radio transmission, Proc. IRE **45,** 794 (1957).

[3] A. H. Allan, D. D. Crombie, and W. A. Penton, Frequency variations in New Zealand of 16 kc/s transmissions from GBR Rugby, Nature **177,** 178 (1956).

[4] W. D. George, NBS Boulder Laboratories. Informal communication.

[5] W. Q. Crichlow, D. F. Smith, R. N. Morton, and W. R. Corliss, Worldwide radio noise levels expected in the frequency band 10 kilocycles to 100 megacycles, NBS Circ. 557 (1955).

[6] Proc. IRE **45,** 6 (1957), vlf issue.

[7] J. R. Wait, The mode theory of vlf ionospheric propagation for finite ground conductivity, Proc. IRE **45,** 760 (1957).

[8] H. J. Round, T. L. Eckersley, K. Tremellen and F. C. Lunnon, Report on measurements made on signal strength at great distances during 1922 and 1923 by an expedition sent to Australia, J. Inst. Elec. Engrs. (London) **63,** 933 (1925).

[9] J. A. Pierce, Sky wave field intensity I. Low and very low frequencies, Cruft Laboratory, Harvard U., Technical Report 158, Sept. 1, 1952.

[10] J. L. Heritage and S. Weisbrod, A study of signal versus distance data at vlf, Symposium on the propagation of vlf radio waves, Boulder, Colo., Jan. 1957, Vol. III.

[11] J. R. Wait, An extension to the mode theory of vlf ionospheric propagation, J. Geophys. Research **63,** 125 (1958).

[12] A. D. Watt, and E. L. Maxwell, Characteristics of atmospheric noise from 1 to 100 kc, Proc. IRE **45,** 787 (1957).

[13] W. L. Taylor, and L. J. Lange, Some Characteristics of vlf propagation using atmospheric waveforms, Proceedings of the second conference on Atmospheric Electricity at Portsmouth, N.H., May, 1958 (Pergamon Press).

[14] A. D. Watt, and E. L. Maxwell, Measured statistical characteristics of vlf atmospheric radio noise, Proc. IRE **45,** 55 (1957).

[15] A. D. Watt, R. M. Coon, E. L. Maxwell, and R. W. Plush, Performance of some radio systems in the presence of thermal and atmospheric noise, Proc. IRE **46,** 1914 (1958).
[16] K. A. Norton, Transmission loss in radio propagation II, to be published.
[17] P. G. Redgment and D. W. Watson, Phase-correlation of medium and very-low-frequency waves using a baseline of several wavelengths, Admiralty Signal and Radar Est., Lythe Hill House, Haslemere, Surrey, England, Monograph No. 836, October, 1948.
[18] R. H. Doherty, NBS Boulder Laboratories. Informal communication.
[19] E. F. Florman, NBS Boulder Laboratories. Informal communication.
[20] D. G. Brennan and M. Lindeman Phillips, Phase and amplitude variability in medium-frequency ionospheric transmission, Technical Report No. 93, Massachusetts Institute of Technology Lincoln Laboratory, September (1957).
[21] J. R. Carson, Notes on the theory of modulation, Proc. IRE **10,** 57 (1922).
[22] A. D. Watt, Statistical characteristics of sampled and integrated A-M and F-M noise, NRL Report 3856 (Oct. 22, 1951).
[23] R. A. Helliwell and E. Gehrels, Observations of magneto-ionic duct propagation using man-made signals of very low frequency, Proc. IRE **46,** 785 (1958).
[24] K. A. Norton, E. L. Shultz, and Helen Yarbrough, The probability distribution of the phase of the resultant vector sum of a constant vector plus a Rayleigh distributed vector, J. Appl. Phys. **23,** 137 (1952).
[25] J. R. Wait, A study of vlf field strength data—both old and new, Geofisica pura e applicata **41** 73 (1958/III).

Boulder, Colo. (Paper 63D1–6)